Progress In Electromagnetics Research Letters, Vol. 25, 67–75, 2011

DUAL-BAND LOW PROFILE DIRECTIONAL ANTENNA WITH HIGH IMPEDANCE SURFACE REFLECTOR

X. Mu*, W. Jiang, S.-X. Gong, and F.-W. Wang

Science and Technology on Antenna and Microwave Laboratory, Xidian University, Xi'an, Shaanxi 710071, China

Abstract—A compact dual-band high impedance surface (HIS) electromagnetic band-gap (EBG) structure is designed as a reflector for a dual-band coplanar waveguide (CPW)-fed planar monopole antenna. The reflector comprises an array of metal square patches which are etched square ring slots. Details of the HIS structure and dual reflection phase frequency bands characteristics are presented and discussed. The simulated and measured results show that the combination of the HIS reflector and the antenna provides directional properties for both frequency bands. At the same time, compared to the antenna integrated with a metal reflector, the profile of the proposed antenna is reduced by more than 60%; the radiation efficiency is increased by 23% (simulated result); and the front-back ratio is increased by 17 dB and 11 dB at the two operating frequency bands, respectively.

1. INTRODUCTION

Planar monopole antennas are widely used in a variety of areas due to the advantages of simple structure, easy fabrication, and low profile [1–3]. But these antennas usually have bidirectional radiation pattern and low gain. Hence, they need to be integrated with a reflector to achieve directional radiation characteristic [4, 5]. It was reported that the metal cavity reflector had been used to provide directional patterns [6], but this kind of antenna is not convenient to use because of its large size.

EBG structures are artificial periodic structures that can be made by metallic or dielectric elements. They are usually used to control the propagation of electromagnetic wave in some range of frequency [7, 8].

Received 11 May 2011, Accepted 9 July 2011, Scheduled 17 July 2011

* Corresponding author: Xin Mu (jupitermx@126.com).

This paper focuses on the reflection phase feature of the EBG surface and low profile antenna. The reflection phase is defined as the phase of the reflected electric field at the reflecting surface. It is known that the perfect electric conductor (PEC) surface has 180° reflection phase, while the perfect magnetic conductor (PMC) surface has 0° reflection phase. However, the EBG surface is different from the two surfaces. The reflection phase of EBG surface varies continuously from 180° to −180° versus frequency, and the $+/-90°$ frequency band is called reflection phase frequency band in conventional definition [7]. That is to say, we can put the antenna which resonates at the reflection phase frequency band very close to the EBG reflector rather than a quarter of wavelength above a metal reflector for the directional characteristic. Furthermore, it is difficult to achieve directional characteristic in different operating frequency bands for multi-band antenna when a metal reflector is used [9, 10].

The EBG structures, especially the HIS structures, have narrow reflection phase frequency band [11], so there is a remarkable growth interest in designing wideband and multi-band HIS structures. Some dual-band HIS structures are found in the field of FSS because of similar property [12]. In [13], the modified mushroom-like HIS was proposed and analyzed, and in [14], the traditional square patch was replaced by a new metal patch to generate two reflection phase frequency bands. These methods are effective but with complex structures and difficulty in fabricating.

In this paper, a simple printed HIS structure which can provide two reflection phase frequency bands is proposed and investigated. Moreover, by using this HIS structure as a reflector, the antenna has directional patterns, low profile, high radiation efficiency and high front-back ratio. Measured results show that the proposed antenna can be used as wearable antenna and WLAN base-station antenna.

2. THE DUAL-BAND HIS STRUCTURE

As shown in Fig. 1, the HIS reflector is made of an array of 5×5 metal square patch cells, which are printed on a FR-4 substrate with thickness of 1 mm, relative permittivity of 4.4 and loss tangent of 0.02. The conductivity of the metal which is used in this paper is 5.8×10^7 s/m. A square ring slot is etched in every cell for the purpose of generating two reflection phase frequency bands. The other side of the substrate is the metallic ground plane.

In this paper, all the simulations are done based on High Frequency Structure Simulator (Ansoft HFSS, ver. 12). With the help of periodic boundary condition (PBC), we just need to analyze

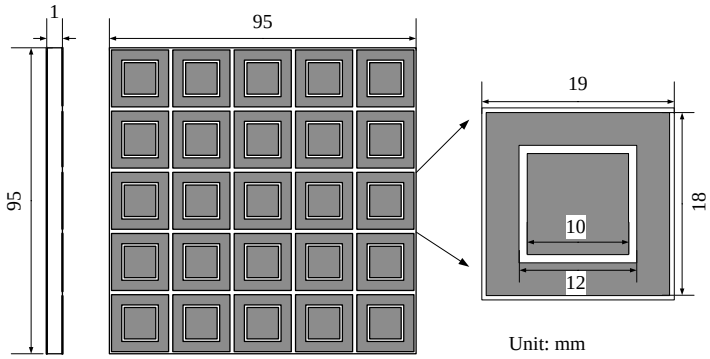

Figure 1. The geometry of the HIS reflector.

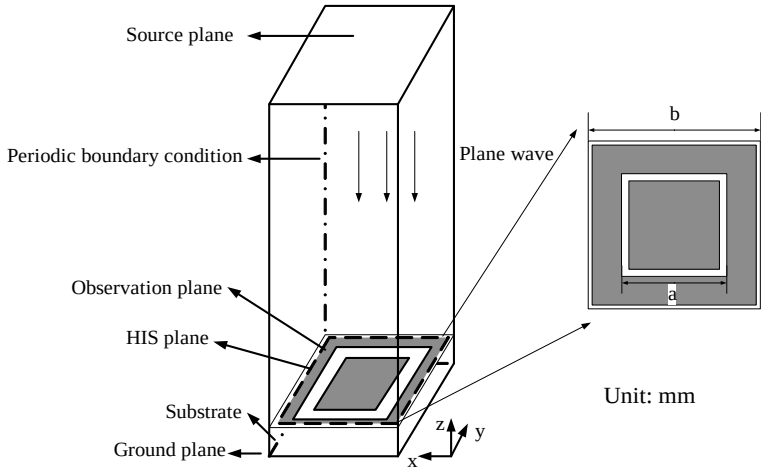

Figure 2. Simulate model for the HIS reflector.

one cell of the HIS reflector to get the reflection phase frequency band of the whole reflector. Fig. 2 shows the model in HFSS. In this model, we put the observation plane very close to the square patch so as to get the reflection phase curves immediately [15].

For further study, the effects of square ring slot and square patch are discussed. Firstly, the effect of a is shown in Fig. 3. The reflection phase curves change slightly in the band of 2.45 GHz while change intensely in the band of 5.2 GHz. The conclusion can be obtained that the values of a mainly affect the reflection phase frequency band at 5.2 GHz.

Secondly, the effect of the size of the square patch is discussed.

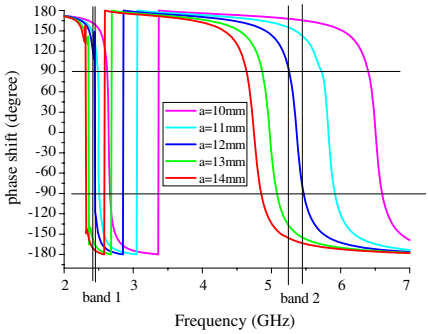

Figure 3. The reflection phase curves for different values of a.

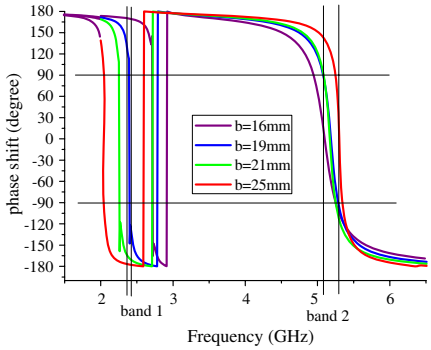

Figure 4. The reflection phase curves for different values of b.

As shown in Fig. 4, the reflection phase curves change significantly in the band of 2.45 GHz while change slightly in the band of 5.2 GHz. We can draw the conclusion that the values of b mainly affect the reflection phase frequency band at 2.45 GHz.

Based on the parameter analysis above, it can be concluded that the values of a affect the high frequency band while the values of b affect the low frequency band. With this conclusion, the HIS reflector is designed by optimized values of $a = 12$ mm, $b = 19$ mm. As we can see in Fig. 3 and Fig. 4, the reflection phase frequency band of this HIS surface is very narrow. (about 20 MHz in the frequency band of 2.45 GHz and 80 MHz in the frequency band of 5.2 GHz).

3. GEOMETRIC ARRANGEMENT FOR ANTENNA WITH HIS REFLECTOR

The geometry of the dual-band antenna is shown in Fig. 5. The two radiation arms are fed by a 50 Ω CPW. The antenna is printed on a FR-4 substrate with thickness of 1.6 mm. The parameters of the antenna structure are shown in Fig. 5 in detail.

The 5×5 HIS array is utilized as a reflector and combined with the proposed antenna. The simulation and measurement models are shown in Fig. 6. The antenna is put in the middle of the reflector and h mm above the reflector. A thin foam layer with thickness of h, relative permittivity of 1.01, and loss tangent of 1.1×10^{-4} is filled between the HIS reflector and the antenna for measurement. This configuration can significantly reduce the spacing between the antenna and the reflector, and provide directional function for both frequency bands.

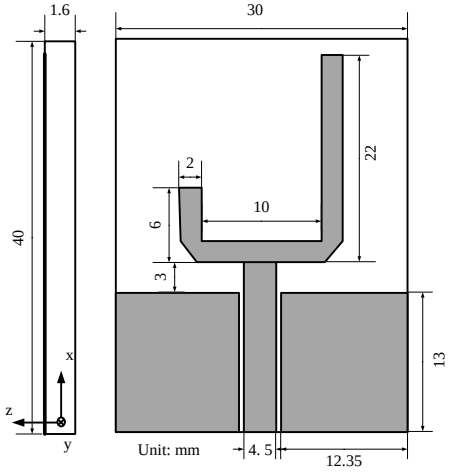

Figure 5. Configuration of the dual-band antenna.

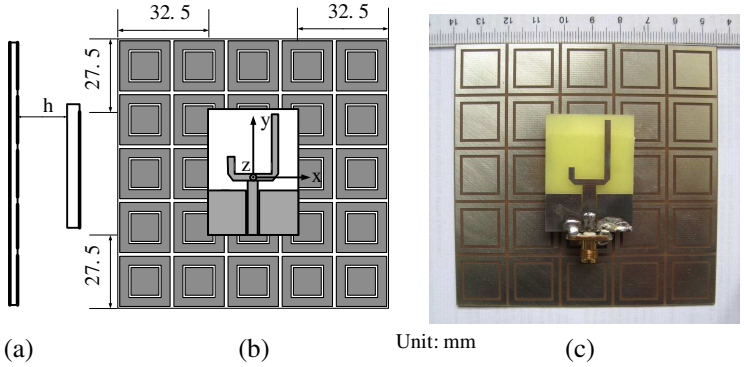

Figure 6. Photograph of the antenna integrated with the HIS reflector. (a), (b) simulation model, (c) measurement model.

4. RESULTS AND DISCUSSION

Figure 7 shows the simulated and measured return losses of the proposed antenna (antenna) and the proposed antenna integrated with the HIS reflector (antenna/HIS). Here we put the proposed antenna 5 mm (about 0.04 wave length) above the HIS reflector. As seen in Fig. 7, the agreement between simulations and measurements is good, for the proposed antenna, the measured 10 dB bandwidths are approximately 280 MHz (2.35 GHz to 2.63 GHz) and 1050 MHz

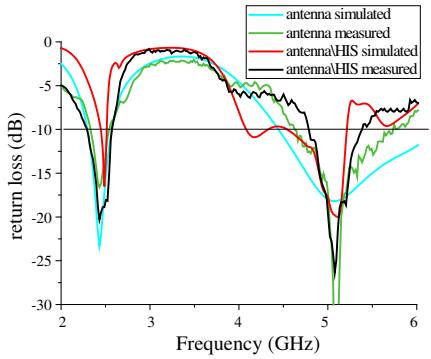

Figure 7. The measured return loss.

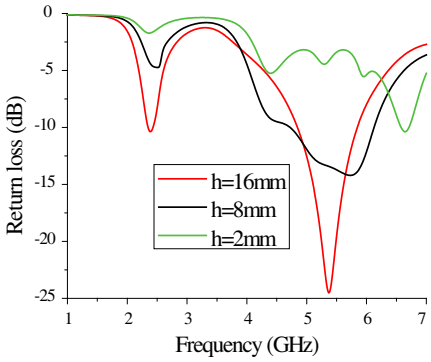

Figure 8. The return loss curves of antenna/PEC.

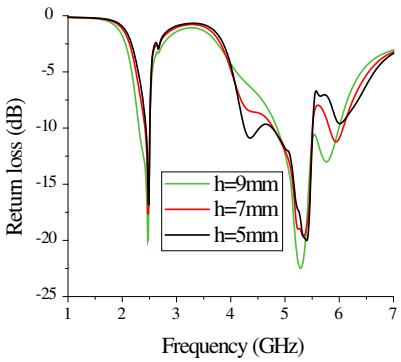

Figure 9. The return loss curves of antenna/HIS.

(4.68 GHz to 5.73 GHz) over the two bands. The measured 10 dB bandwidths for the antenna/HIS are 260 MHz (2.33 GHz to 2.59 GHz) and 590 MHz (4.76 GHz to 5.35 GHz) over the two bands, respectively. Thus, the combination with the HIS reflector causes a decrease in bandwidth, especially in the high frequency band.

For comparison, a similar model that the proposed antenna integrated with a metal reflector (antenna/PEC) is also fabricated and analyzed. Fig. 8 and Fig. 9 show the simulated return loss curves of the antenna/PEC and the antenna/HIS with different values of h. It can be seen that it is hard for the antenna/PEC to work at the two frequency bands properly, and the distance ($+z$ axis) between the antenna and the reflector will be larger than 16 mm (0.13 wave length) for better performance, which is much larger than that of the antenna/HIS. However, the antenna/HIS can work well at the two

frequency bands with smaller h (0.04 wave length), which means that the HIS reflector can reduce the profile of the planar monopole antenna more than 60%. At the same time, the curves in Fig. 9 show an upward shift in frequency as h is reduced. In this case, the h is selected to be 5 mm which leads to a relatively wide bandwidth and low profile.

Antenna radiation pattern measurement has been performed in an anechoic chamber. Fig. 10 and Fig. 11 show the simulated and measured normalized radiation patterns in the E- and H-planes for the antenna/HIS and antenna/PEC. As we can see, the back-lobe of the patterns can be reduced remarkably when the HIS reflector is used. Compared to the antenna/PEC, the front-back ratio can be increased from 25 dB to 42 dB at the band of 2.45 GHz and from 30 dB to 41 dB at the band of 5.2 GHz. The gain can be increased from 5.6 dB to 7.1 dB at the band of 2.45 GHz and from 6.5 dB to 7.8 dB at the band of 5.2 GHz. We can reach the conclusion that the combination with

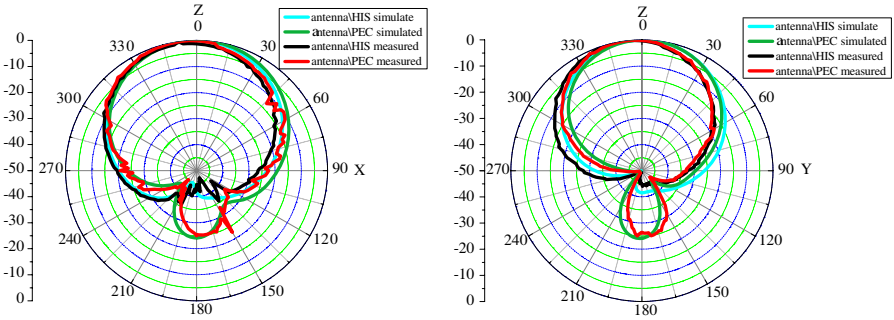

(a) E-plane (b) H-plane

Figure 10. Radiation patterns at 2.45 GHz.

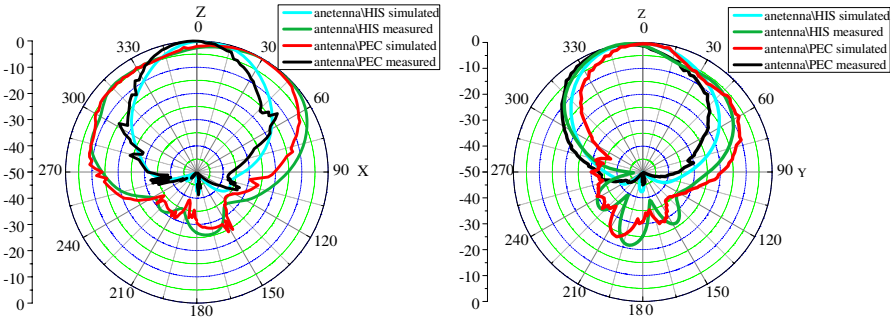

(a) E-plane (b) H-plane

Figure 11. Radiation patterns at 5.2 GHz.

Table 1. Simulated radiation efficiency of the antenna systems.

	antenna	antenna/PEC	antenna/HIS
2.45 GHz	48.5%	58.2%	71.3%
5.2 GHz	52.1%	63.9%	70.9%

the HIS reflector enhances the front-back ratio and the gain of the proposed antenna significantly.

The simulated radiation efficiencies of the antenna systems are given in Table 1.

We can see from the table that the radiation efficiency of the antenna/HIS is higher than that of the antenna/PEC (about 13% improvement) and the antenna (about 23% improvement).

5. CONCLUSION

A compact dual-band HIS-EBG integrated with a dual-band antenna is proposed. Compared to the conventional mushroom-like EBG structure, the proposed HIS has two reflection phase frequency bands with simple structure and easy fabrication. When it is used as a reflector for a dual-band monopole antenna, it provides smaller size, higher gain, higher radiation efficiency and greater front-back ratio than metal reflector over the two frequency bands, but it also causes a reduction of bandwidth, especially in the high frequency band.

REFERENCES

1. Nakano, H., K. Kikkawa, N. Kondo, Y. Iitsuka, and J. Yamauchi, "Low-profile equiangular spiral antenna backed by an EBG reflector," *IEEE Transactions on Antennas and Propagation*, Vol. 57, No. 5, 1309–1318, 2009.
2. Shams, K. M. Z., M. Ali, and H. S. Hwang, "A planar inductively coupled bow-tie slot antenna for WLAN application," *Journal of Electromagnetic Waves and Applications*, Vol. 20, No. 7, 861–871, 2006.
3. Denidni, T. A., Q. Rao, and A. R. Sebak, "T-shaped microstrip feeding technique for a dual annnular slot antenna," *Journal of Electromagnetic Waves and Applications*, Vol. 19, No. 5, 605–614, 2005.
4. Kim, Y., F. Yang, and A. Z. Elsherbeni, "Compact artificial magnetic conductor designs using planar square spiral geometries," *Progress In Electromagnetics Research*, Vol. 77, 43–54, 2007.

5. Gu, Y. Y., W. X. Zhang, and Z. C. Ge, "Two improved Fabry-Perot resonator printed antennas using EBG superstrate and AMC substrate," *Journal of Electromagnetic Waves and Applications*, Vol. 21, No. 6, 719–728, 2007.
6. Qu, S. W., J. L. Li, Q. Xue, and C. H. Chan, "Novel unidirectional slot antenna with a vertical wall," *Progress In Electromagnetics Research*, Vol. 84, 239–251, 2008.
7. Yang, F. and Y. R. Samii, "Reflection phase characterizations of the EBG ground plane for low profile wire antenna applications," *IEEE Transactions on Antennas and Propagation*, Vol. 51, No. 10, 2003.
8. Fu, Y. Q., Q. R. Zheng, Q. Gao, and G. H. Zhang, "Mutual coupling reduction between large antenna arrays using electromagnetic band-gap (EBG) structures," *Journal of Electromagnetic Waves and Applications*, Vol. 20, No. 6, 819–825, 2006.
9. Sohn, J. R., K. Y. Kim, H.-S. Tae, and H. J. Lee, "Comparative study on various artificial magnetic conductors for low-profile antenna," *Progress In Electromagnetics Research*, Vol. 61, 27–37, 2006.
10. Zhu, S. Z. and R. Langley, "Dual-band wearable textile antenna on an EBG substrate," *IEEE Transactions on Antennas and Propagation*, Vol. 57, No. 4, 926–935, 2009.
11. Yang, F., V. Demir, D. A. Elsherbeni, A. Z. Elsherbeni, and A. A. Eldek, "Enhancement of printed dipole antennas characteristics using semi-EBG ground plane," *Journal of Electromagnetic Waves and Applications*, Vol. 20, No. 8, 993–1006, 2006.
12. Hosseini, M., A. Pirhadi, and M. Hakkak, "A novel AMC with little sensitivity to the angle of incidence using 2-layer jerusalem cross FSS," *Progress In Electromagnetics Research*, Vol. 64, 43–51, 2006.
13. Liang, L. C. H. Liang, L. Chen, and X. Chen, "A novel broadband EBG using cascaded mushroom-like structure," *Microwave Optical Technology Letters*, Vol. 50, No. 21, 67–2170, 2008.
14. Zhang, L.-J., C.-H. Liang, L. Liang, and L. Chen, "A novel design approach for dual-band electromagnetic band-gap structure," *Progress In Electromagnetics Research M*, Vol. 4, 81–91, 2008.
15. Yang, F. and Y. R. Samii, *Electromagnetic Band Gap Structures in Antenna Engineering*, Cambridge University Press, 2009.